New Journal of Physics
The open-access journal for physics

# Rabi oscillations in a qubit coupled to a quantum two-level system

**S Ashhab**[1], **J R Johansson**[1] **and Franco Nori**[1,2]

[1] Frontier Research System, The Institute of Physical and Chemical Research (RIKEN), Wako-shi, Saitama 351-0198, Japan
[2] Center for Theoretical Physics, CSCS, Department of Physics, University of Michigan, Ann Arbor, MI 48109-1040, USA
E-mail: ashhab@riken.jp

*New Journal of Physics* **8** (2006) 103
Received 24 February 2006
Published 16 June 2006
Online at http://www.njp.org/
doi:10.1088/1367-2630/8/6/103

**Abstract.** We consider the problem of a qubit driven by a harmonically oscillating external field while it is coupled to a quantum two-level system (TLS). We perform a systematic numerical analysis of the problem by varying the relevant parameters. The numerical calculations agree with the predictions of a simple intuitive picture, namely one that takes into consideration the four-level energy spectrum, the simple principles of Rabi oscillations and the basic effects of decoherence. Furthermore, they reveal a number of other interesting phenomena. We provide explanations for the various features that we observe in the numerical calculations and discuss how they can be used in experiment. In particular, we suggest an experimental procedure to characterize an environment of TLSs.


PII: S1367-2630(06)19414-8

## Contents



## 1. Introduction

There have been remarkable advances in the field of superconductor-based quantum information processing in recent years (there are now several reviews on the subject, see e.g. [1]). Coherent oscillations and basic gate operations have been observed in systems of single qubits and two interacting qubits [2]–[9]. One of the most important operations that are used in manipulating qubits is the application of an oscillating external field on resonance with the qubit to drive Rabi oscillations [3]–[6], [10]. A closely related problem with great promise of possible applications is that of a qubit coupled to a quantum harmonic-oscillator mode [11]–[14].

Qubits are always coupled to uncontrollable degrees of freedom that cause decoherence in its dynamics. One generally thinks of the environment as slowly reducing the coherence of the qubit, typically as a monotonically decreasing decay function. In some recent experiments, however, oscillations in the qubit have been observed that imply it is strongly coupled to quantum degrees of freedom with long decoherence times [10, 15]. The effects of those degrees of freedom have been successfully described by modelling them as quantum two-level systems (TLSs) [16]–[20]. Since, as mentioned above, Rabi oscillations are a simple and powerful method to manipulate the quantum state of a qubit, it is important to understand the behaviour of a qubit that is driven on or close to resonance in the presence of such a TLS. Furthermore, we shall show below that driving the qubit close to resonance can be used to extract more parameters about an environment of TLSs than has been done in experiment so far. The results of this study are also relevant to the problem of Rabi oscillations in a qubit that is interacting with other surrounding qubits.

Some theoretical treatments and analysis of special cases of the problem at hand were given in [15, 19]. In this paper, we perform a more systematic analysis in order to reach a more complete understanding of this phenomenon. We shall present a few simple physical principles that can be used to understand several aspects of the behaviour of this system with different possible choices of the relevant parameters. Those principles are (1) the four-level energy spectrum of the qubit+TLS system, (2) the basic properties of the Rabi-oscillation dynamics and (3) the basic

effects of decoherence. We shall then perform numerical calculations that will agree with that intuitive picture and also will reveal other results that are more difficult to definitively predict otherwise. Finally, we suggest an experimental procedure where the driven qubit dynamics can be used to characterize the environment of TLSs.

The paper is organized as follows: in section 2, we introduce the model system and the Hamiltonian that describes it. In section 3, we present a few simple arguments that will be used as a foundation for our numerical analysis of section 4, which will confirm that intuitive picture and reveal other less intuitively predictable results (note that a reader who is sufficiently familiar with the subject matter can skip section 3). In section 5, we discuss how our results can be used in experiment. We finally conclude our discussion in section 6.

## 2. Model system

The model system that we shall study in this paper is composed of a harmonically driven qubit, a quantum TLS and their weakly coupled environment.[3] We assume that the qubit and the TLS interact with their own (uncorrelated) environments that would cause decoherence even in the absence of qubit–TLS coupling. The Hamiltonian of the system is given by:

$$\hat{H}(t) = \hat{H}_{\mathrm{q}}(t) + \hat{H}_{\mathrm{TLS}} + \hat{H}_{\mathrm{I}} + \hat{H}_{\mathrm{Env}}, \tag{1}$$

where $\hat{H}_{\mathrm{q}}$ and $\hat{H}_{\mathrm{TLS}}$ are the qubit and TLS Hamiltonians, respectively; $\hat{H}_{\mathrm{I}}$ describes the coupling between the qubit and the TLS, and $\hat{H}_{\mathrm{Env}}$ describes all the degrees of freedom in the environment and their coupling to the qubit and TLS. The (time-dependent) qubit Hamiltonian is given by:

$$\hat{H}_{\mathrm{q}}(t) = -\frac{\Delta_{\mathrm{q}}}{2}\hat{\sigma}_x^{(\mathrm{q})} - \frac{\epsilon_{\mathrm{q}}}{2}\hat{\sigma}_z^{(\mathrm{q})} + F\cos(\omega t)\left(\sin\theta_{\mathrm{f}}\hat{\sigma}_x^{(\mathrm{q})} + \cos\theta_{\mathrm{f}}\hat{\sigma}_z^{(\mathrm{q})}\right), \tag{2}$$

where $\Delta_{\mathrm{q}}$ and $\epsilon_{\mathrm{q}}$ are the adjustable static control parameters of the qubit, $\hat{\sigma}_\alpha^{(\mathrm{q})}$ are the Pauli spin matrices of the qubit, $F$ and $\omega$ are the amplitude (in energy units) and frequency, respectively, of the driving field, and $\theta_{\mathrm{f}}$ is an angle that describes the orientation of the external field relative to the qubit $\hat{\sigma}_z$ axis. Although we have used a rather general form to describe the coupling between the qubit and the driving field, we shall see in section 3 that one only needs a single, easily extractable parameter to characterize the amplitude of the driving field. We assume that the TLS is not coupled to the external driving field, and its Hamiltonian is given by:

$$\hat{H}_{\mathrm{TLS}} = -\frac{\Delta_{\mathrm{TLS}}}{2}\hat{\sigma}_x^{(\mathrm{TLS})} - \frac{\epsilon_{\mathrm{TLS}}}{2}\hat{\sigma}_z^{(\mathrm{TLS})}, \tag{3}$$

where the definition of the parameters and operators is similar to those of the qubit, except that the TLS parameters are uncontrollable. Note that our assumption that the TLS is not coupled to the driving field can be valid even in cases where the physical nature of the TLS and the

[3] We shall make a number of assumptions that might seem too specific at certain points. We have been careful, however, not to make a choice of parameters that causes any of the interesting physical phenomena to disappear. For a more detailed discussion of our assumptions, see [20].

driving field leads to such coupling, since we generally consider a microscopic TLS, rendering any coupling to the external field negligible.

The energy splitting between the two quantum states of each subsystem, in the absence of coupling between them, is given by:

$$E_\alpha = \sqrt{\Delta_\alpha^2 + \epsilon_\alpha^2}, \tag{4}$$

where the index $\alpha$ refers to either the qubit or the TLS. The corresponding ground and excited states are, respectively, given by:

$$|g\rangle_\alpha = \cos\frac{\theta_\alpha}{2}|\uparrow\rangle_\alpha + \sin\frac{\theta_\alpha}{2}|\downarrow\rangle_\alpha, \qquad |e\rangle_\alpha = \sin\frac{\theta_\alpha}{2}|\uparrow\rangle_\alpha - \cos\frac{\theta_\alpha}{2}|\downarrow\rangle_\alpha, \tag{5}$$

where the angle $\theta_\alpha$ is given by the criterion $\tan\theta_\alpha = \Delta_\alpha/\epsilon_\alpha$. We take the interaction Hamiltonian between the qubit and the TLS to be of the form:

$$\hat{H}_\mathrm{I} = -\frac{\lambda}{2}\hat{\sigma}_z^{(\mathrm{q})} \otimes \hat{\sigma}_z^{(\mathrm{TLS})}, \tag{6}$$

where $\lambda$ is the (uncontrollable) coupling strength between the qubit and the TLS. Note that any interaction Hamiltonian that is a product of a qubit observable times a TLS observable can be recast into the above form using a simple basis transformation, keeping in mind that such a basis transformation also changes the values of $\theta_\mathrm{q}$, $\theta_\mathrm{TLS}$ and $\theta_\mathrm{f}$.

We assume that all the coupling terms in $\hat{H}_\mathrm{Env}$ are small enough that its effect on the dynamics of the qubit+TLS system can be treated within the framework of the markovian Bloch–Redfield master equation approach. We shall use a noise power spectrum that can describe both dephasing and relaxation with independently adjustable rates, and we shall present our results in terms of those decoherence rates. For definiteness in the numerical calculations, we take the coupling of the qubit and the TLS to their respective environments to be described by the operators $\hat{\sigma}_z^{(\alpha)}$, where $\alpha$ refers to the qubit and the TLS. Note, however, that since we use the relaxation and dephasing rates to quantify decoherence, our results are independent of the choice of system–environment coupling operators.

## 3. Intuitive picture

We start our analysis of the problem by presenting a few physical principles that prove very helpful in intuitively predicting the behaviour of the above-described system. Note that the arguments given in this section are well known [21, 22, 23]. For the sake of clarity, however, we present them explicitly and discuss their roles in the problem at hand.

### *3.1. Energy levels and eigenstates*

The first element that one needs to consider is the energy levels of the combined qubit+TLS system. In order for a given experimental sample to function as a qubit, the qubit–TLS coupling strength $\lambda$ must be much smaller than the energy splitting of the qubit $E_\mathrm{q}$. We therefore take that

limit, as well as the limit $\lambda \ll E_{\mathrm{TLS}}$, and straightforwardly find the energy levels to be given by

$$E_1 = -\frac{E_{\mathrm{TLS}} + E_{\mathrm{q}}}{2} - \frac{\lambda_{\mathrm{cc}}}{2}, \qquad E_2 = -\frac{1}{2}\sqrt{\left(E_{\mathrm{TLS}} - E_{\mathrm{q}}\right)^2 + \lambda_{\mathrm{ss}}^2} + \frac{\lambda_{\mathrm{cc}}}{2},$$
$$E_3 = +\frac{1}{2}\sqrt{\left(E_{\mathrm{TLS}} - E_{\mathrm{q}}\right)^2 + \lambda_{\mathrm{ss}}^2} + \frac{\lambda_{\mathrm{cc}}}{2}, \qquad E_4 = +\frac{E_{\mathrm{TLS}} + E_{\mathrm{q}}}{2} - \frac{\lambda_{\mathrm{cc}}}{2}, \tag{7}$$

where $\lambda_{\mathrm{cc}} = \lambda \cos\theta_{\mathrm{q}} \cos\theta_{\mathrm{TLS}}$, $\lambda_{\mathrm{ss}} = \lambda \sin\theta_{\mathrm{q}} \sin\theta_{\mathrm{TLS}}$. The corresponding eigenstates are given by:

$$|1\rangle = |gg\rangle, \qquad |2\rangle = \cos\frac{\varphi}{2}|eg\rangle + \sin\frac{\varphi}{2}|ge\rangle, \qquad |3\rangle = \sin\frac{\varphi}{2}|eg\rangle - \cos\frac{\varphi}{2}|ge\rangle, \qquad |4\rangle = |ee\rangle, \tag{8}$$

where the first symbol refers to the qubit state and the second one refers to the TLS state in their respective uncoupled bases, the angle $\varphi$ is given by the criterion $\tan\varphi = \lambda_{\mathrm{ss}}/(E_{\mathrm{TLS}} - E_{\mathrm{q}})$, and for definiteness in the form of the states $|2\rangle$ and $|3\rangle$ we have assumed that $E_{\mathrm{TLS}} \geqslant E_{\mathrm{q}}$.

Note that the mean-field shift of the qubit resonance frequency, $\lambda_{\mathrm{cc}}$, is present regardless of the values of the qubit and TLS energy splittings. The avoided-crossing structure involving states $|2\rangle$ and $|3\rangle$, however, is only relevant when the qubit and TLS energies are almost equal. One can therefore use spectroscopy of the four-level structure to experimentally measure the TLS energy splitting $E_{\mathrm{TLS}}$ and angle $\theta_{\mathrm{TLS}}$, as will be discussed in more detail in section 5.

### *3.2. Rabi oscillations*

If a TLS (e.g. a qubit) with energy splitting $\omega_0$, initially in its ground state, is driven by a harmonically oscillating weak field with a frequency $\omega$ close to its energy splitting (up to a factor of $\hbar$) as described by equation (3), its probability to be found in the excited state at a later time $t$ is given by:

$$P_{\mathrm{e}} = \frac{\Omega_0^2}{\Omega_0^2 + (\omega - \omega_0)^2}\frac{1 - \cos(\Omega t)}{2}, \tag{9}$$

where $\Omega = \sqrt{\Omega_0^2 + (\omega - \omega_0)^2}$, and the on-resonance Rabi frequency $\Omega_0 = F|\sin(\theta_{\mathrm{f}} - \theta_{\mathrm{q}})|$ (we take $\hbar = 1$) [23]. We therefore see that maximum oscillations with full $g \leftrightarrow e$ conversion probability are obtained when the driving is resonant with the qubit energy splitting. We also see that the width of the Rabi peak in the frequency domain is given by $\Omega_0$. Simple Rabi oscillations can also be observed in a multi-level system if the driving frequency is on resonance with one of the relevant energy splittings but off resonance with all others.

### *3.3. The effect of decoherence*

In an undriven system, the effect of decoherence is to push the density matrix describing the system towards its thermal-equilibrium value with timescales given by the characteristic dephasing and relaxation times. The effects of decoherence, especially dephasing, can be thought of in terms of a broadening of the energy levels. In particular, if the energy separation between the states $|2\rangle$ and $|3\rangle$ of subsection 3.1 is smaller than the typical decoherence rates in the problem,

any effect related to that energy separation becomes unobservable. Alternatively, one could say that only processes that occur on a timescale faster than the decoherence times can be observed.

It is worth taking a moment to look in some more detail at the problem of a resonantly driven qubit coupled to a dissipative environment, which is usually studied under the name of Bloch-equations [23].[4] If the Rabi frequency is much smaller than the decoherence rates, the qubit will remain in its thermal equilibrium state, since any deviations from that state caused by the driving field will be dissipated immediately. If, on the other hand, the Rabi frequency is much larger than the decoherence rates, the system will perform damped Rabi oscillations, and it will end up close to the maximally mixed state in which both states $|g\rangle$ and $|e\rangle$ have equal occupation probability. In that case, one could say that decoherence succeeds in making us lose track of the quantum state of the qubit but fails to dissipate the energy of the qubit, since more energy will always be available from the driving field.

### *3.4. Combined picture*

We now take the three elements presented above and combine them to obtain a simple intuitive picture of the problem at hand.

Let us for a moment neglect the effects of decoherence and only consider the case $\omega \approx \omega_0$. The driving field tries to flip the state of the qubit alone. However, two of the relevant eigenstates are entangled states, namely $|2\rangle$ and $|3\rangle$. One can therefore expect that if the width of the Rabi peak, or in other words the on-resonance Rabi frequency, is much larger than the energy separation between the states $|2\rangle$ and $|3\rangle$, the qubit will start oscillating much faster than the TLS can respond, and the initial dynamics will look similar to that of the uncoupled system. Only after many oscillations and a time of the order of $(E_3 - E_2)^{-1}$ will one start to see the effects of the qubit-TLS interaction. If, on the other hand, the Rabi frequency is much smaller than the energy separation between the states $|2\rangle$ and $|3\rangle$, the driving field can excite at most one of those two states, depending on the driving frequency. In that case the qubit-TLS interactions are strong enough that the TLS can follow adiabatically the time evolution of the qubit. In the intermediate region, one expects that if the driving frequency is closer to one of the two transition frequencies $E_2 - E_1$ and $E_3 - E_1$, beating behaviour will be seen right from the beginning. If one looks at the Rabi peak in the frequency domain, e.g. by plotting the maximum $g \leftrightarrow e$ qubit-state conversion probability as a function of frequency, the single peak of the weak-coupling limit separates into two peaks as the qubit–TLS coupling strength becomes comparable to and exceeds the on-resonance Rabi frequency.

We do not expect weak to moderate levels of decoherence to cause any qualitative changes in the qubit dynamics other than, for example, imposing a decaying envelope on the qubit excitation probability. As mentioned above, features that are narrower (in frequency) than the decoherence rates will be suppressed the most. Note that if the TLS decoherence rates are large enough [20], the TLS can be neglected and one recovers the single Rabi peak with a height determined by the qubit decoherence rates alone.

## 4. Numerical results

In the absence of decoherence, we find it easiest to treat the problem at hand using the dressed-state picture [22]. In that picture one thinks of the driving field mode as being quantized, and

[4] For studies of certain aspects of this problem in superconducting qubits see [24].

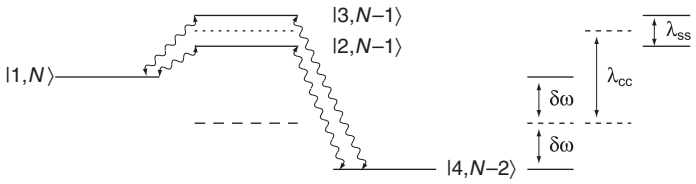


**Figure 1.** Left: energy levels and direct transitions between them in the dressed-state picture. Right: energy splittings separated according to their physical origin.

processes are described as involving the absorption and emission of quantized photons by the qubit+TLS combined system. We take the frequency of the driving field to be close to the qubit and TLS energy splittings. For simplicity, we take those to be equal. We shall come back to the general case later in this section. Without going over the rather simple details of the derivation, we show the four relevant energy levels and the possible transitions in figure 1. The effective Hamiltonian describing the dynamics within those four levels is given by:

$$\hat{H}_{\text{eff}} = \begin{pmatrix} 0 & \Omega_0' & \Omega_0' & 0 \\ \Omega_0' & -\delta\omega + \lambda_{\text{cc}} - \lambda_{\text{ss}}/2 & 0 & \Omega_0' \\ \Omega_0' & 0 & -\delta\omega + \lambda_{\text{cc}} + \lambda_{\text{ss}}/2 & -\Omega_0' \\ 0 & \Omega_0' & -\Omega_0' & -2\delta\omega \end{pmatrix} \tag{10}$$

where $\Omega_0' = \Omega_0/2^{3/2}$, $\Omega_0$ is the on-resonance Rabi frequency in the absence of qubit–TLS coupling, $\delta\omega = \omega - \omega_0$, and the Hamiltonian is expressed in the basis of states ($|1, N\rangle$, $|2, N-1\rangle$, $|3, N-1\rangle$ and $|4, N-2\rangle$), where $N$ is the number of photons in the driving field. We take the low temperature limit, which means that we can take the initial state to be $|1, N\rangle$ without the need for any extra initialization. We can now evolve the system numerically and analyse the dynamics. After we find the density matrix of the combined qubit+TLS system as a function of time, we can look at the dynamics of the combined system or that of the two subsystems separately, depending on which one provides more insightful information.

We start by demonstrating the separation of the Rabi peak into two peaks as the qubit–TLS coupling strength is increased. As a quantifier of the amplitude of Rabi oscillations, we use the maximum probability for the qubit to be found in the excited state between times $t = 0$ and $t = 20\pi/\Omega_0$, and we refer to that quantity as $P^{(\text{q})}_{\uparrow,\text{max}}$. In figure 2, we plot $P^{(\text{q})}_{\uparrow,\text{max}}$ as a function of renormalized detuning $\delta\omega/\Omega_0$. As was explained in section 3, the peak separates into two when the qubit–TLS coupling strength exceeds the on-resonance Rabi frequency, up to simple factors of order one. The system also behaves according to the explanation given in section 3 in the weak- and strong-coupling limits. When $\lambda$ is substantially smaller than $\Omega_0$, oscillations in the qubit state occur on a timescale $\Omega^{-1}$, where $\Omega$ is the Rabi frequency defined in subsection 3.2, whereas the beating behaviour occurs on a timescale $(E_3 - E_2)^{-1}$. When $\lambda$ is more than an order of magnitude smaller than $\Omega_0$, the effects of the TLS are hardly visible in the qubit dynamics within the time given above. On the other hand, when $\lambda$ is large enough such that the energy difference $E_3 - E_2$ is several times larger than $\Omega_0$, the dynamics corresponds to exciting at most one of the two eigenstates $|2\rangle$ and $|3\rangle$. We generally see that beating behaviour becomes less pronounced when the driving frequency is equal to the qubit energy splitting including the

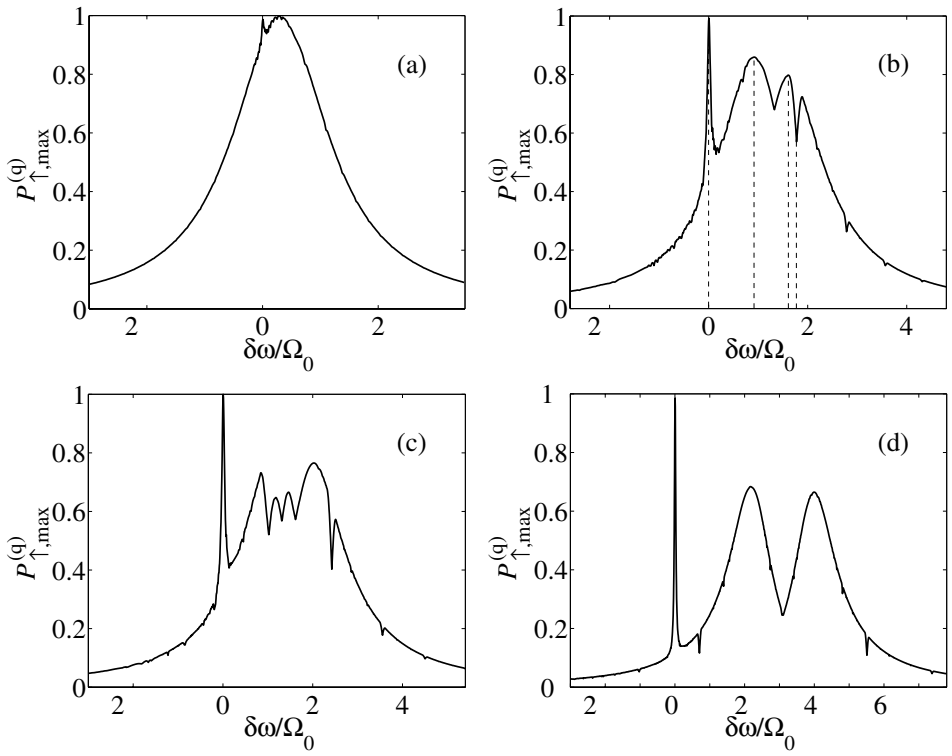


**Figure 2.** Maximum qubit excitation probability $P^{(q)}_{\uparrow,max}$ between $t = 0$ and $t = 20\pi/\Omega_0$ for $\lambda/\Omega_0 = 0.5$ (a), 2 (b), 2.5 (c) and 5 (d). $\theta_q = \pi/4$ and $\theta_{TLS} = \pi/6$.

TLS-mean-field shift, i.e. when $\omega = \sqrt{\Delta_q^2 + (\epsilon_q + \lambda_{cc})^2}$, which corresponds to the top of the unsplit single peak or the midpoint between the two separated peaks.

We also see some interesting features in the peak structure of figure 2 that were not discussed in section 3. In the intermediate-coupling regime (figures 2(b) and (c)), we see a peak that reaches unit height, i.e. a peak that corresponds to full $g \leftrightarrow e$ conversion in the qubit dynamics at $\delta\omega = 0$. The asymmetry between the two main peaks in figure 2, as well as the additional dips in the double-peak structure, were also not immediately obvious from the simple arguments of section 3. In order to give a first explanation of the above features, we plot in figure 3 a curve similar to that in figure 2(b) (with different $\theta_{TLS}$), along with the same quantity plotted when the eigenstate $|4, N-2\rangle$ is neglected, i.e. by using a reduced $3 \times 3$ Hamiltonian where the fourth row and column are removed from $\hat{H}_{eff}$. In the three-state calculation, there is no $\delta\omega = 0$ peak, the two main peaks are symmetric, but we still see some dips. We also plot in figure 4 the qubit excitation probability as a function of time for the four frequencies marked by vertical dashed lines in figure 2(b).

By looking at figure 1, one might say that the $\delta\omega = 0$ peak clearly corresponds to a two-photon process coupling states $|1\rangle$ and $|4\rangle$. In fact, for further demonstration that this is the case, we have included in figure 4 the probability of the combined qubit+TLS system to be in state $|4\rangle$. This peak is easiest to observe in the intermediate coupling regime. In the weak-coupling limit, the qubit and TLS are essentially decoupled, especially on the timescale of qubit dynamics. In the strong coupling limit, one can argue that a Raman transition will give rise to that peak. However, noting that the width of that peak is of the order of the smaller of the

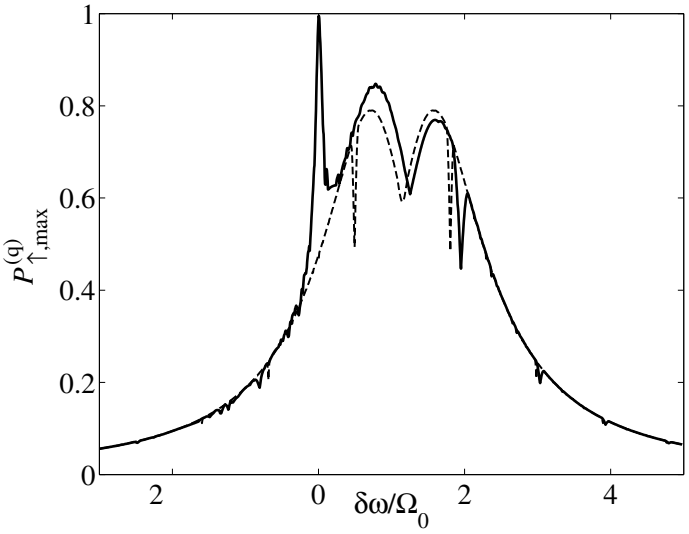


**Figure 3.** Maximum qubit excitation probability $P^{(q)}_{\uparrow,\max}$ between $t = 0$ and $t = 20\pi/\Omega_0$ for the four-level system (solid line) and the reduced three-level system (dashed line). $\lambda/\Omega_0 = 2$, $\theta_q = \pi/4$ and $\theta_{TLS} = \pi/5$.

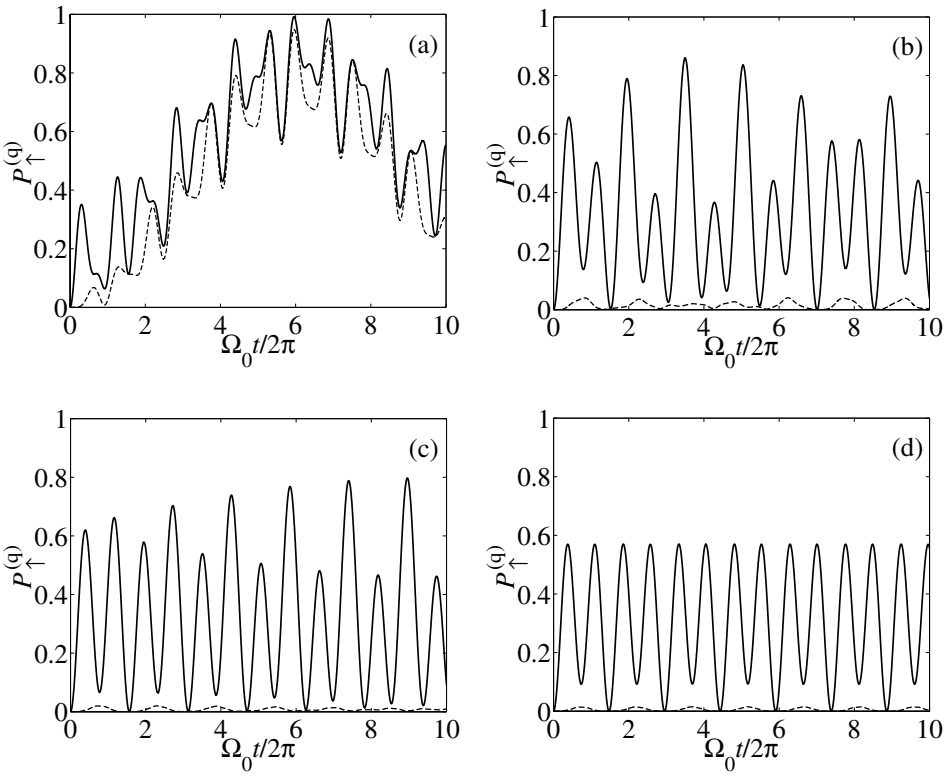


**Figure 4.** Qubit excitation probability $P^{(q)}_{\uparrow}$ as a function of time (solid line) for $\delta\omega/\Omega_0 = 0$ (a), 0.92 (b), 1.61 (c) and 1.77 (d). The dashed line is the occupation probability of state $|4, N-2\rangle$. $\lambda/\Omega_0 = 2$, $\theta_q = \pi/4$ and $\theta_{TLS} = \pi/5$.

values $\Omega_0^2/\lambda_{ss}$ and $\Omega_0^2/\lambda_{cc}$, we can see that it becomes increasingly narrow in that limit. In other words, the virtual intermediate state after the absorption of one photon is far enough in energy from the states $|2\rangle$ and $|3\rangle$ to make the peak invisibly narrow. It is rather surprising, however, that in the intermediate-coupling regime the peak reaches unit $g \leftrightarrow e$ conversion probability, even though the transitions to states $|2\rangle$ and $|3\rangle$ are real, rather than being virtual transitions whose role is merely to mediate the coupling between states $|1\rangle$ and $|4\rangle$. We have verified that the (almost) unit height of the peak is quite robust against changes in the angles $\theta_q$ and $\theta_{TLS}$ for a wide range in $\lambda$, even when that peak coincides with the top of one of the two main peaks. In fact, the Hamiltonian $\hat{H}_{eff}$ can be diagonalized rather straightforwardly in the case $\delta\omega = 0$, and one can see that there is no symmetry that requires full conversion between the states $|1, N\rangle$ and $|4, N-2\rangle$. The lack of any special relations between the energy differences in the eigenvalues of $\hat{H}_{eff}$, however, suggests that almost full conversion should be achieved in a reasonable amount of time.

The asymmetry between the two main peaks in figures 2 and 3 can also be explained by the fact that in one of those peaks state $|4\rangle$ is also involved in the dynamics and it increases the quantity $P^{(q)}_{\uparrow,max}$. As above, we have included in figures 4(b) and (c) the probability of the combined qubit+TLS system to be in state $|4\rangle$.

In order to explain the dips in figures 2 and 3, we note that the plotted quantity, $P^{(q)}_{\uparrow,max}$, is the sum of four terms (in the reduced three-level system): a constant and three oscillating terms. The frequencies of those terms correspond to the energy differences in the diagonalized $3 \times 3$ Hamiltonian. The dips occur at frequencies where the two largest frequencies are integer multiples of the smallest one. Away from any such point, $P^{(q)}_{\uparrow,max}$ will reach a value equal to the sum of the amplitudes of the four terms. Exactly at those points, however, such a constructive build-up of amplitudes is not always possible, and a dip is generally obtained. The width of that dip decreases and vanishes asymptotically as we increase the simulation time, although the depth remains unaffected.

We also studied the case where the qubit and TLS energy splittings were different. As can be expected, the effects of the TLS decrease as it moves away from resonance with the qubit. That is most clearly reflected in the two-peak structure, where one of the two main peaks becomes substantially smaller than the other. The two-photon peak was still clearly observable in plots corresponding to the same quantity plotted in figure 2, i.e. plots of $P^{(q)}_{\uparrow,max}$ versus $\delta\omega/\Omega_0$, even when the detuning between the qubit and the TLS was a few times larger than the coupling strength and the on-resonance Rabi frequency.

The truncated dressed-state picture with four energy levels is insufficient to study the effects of decoherence. For example, relaxation from state $|2\rangle$ to $|1\rangle$ does not necessarily have to involve emission of a photon into the driving-field mode. We therefore study the effects of decoherence by treating the driving field classically. We then solve a Bloch–Redfield master equation with a time-dependent Hamiltonian and externally imposed dephasing and relaxation times, as was done in [20]. In figure 5 we reproduce the four-level results of figure 3, i.e. $P^{(q)}_{\uparrow,max}$ versus $\delta\omega/\Omega_0$ with no decoherence, along with the same quantity obtained when we take into account the effects of decoherence. For a moderate level of decoherence, we see that the qubit excitation probability is somewhat reduced and all the features that are narrower than the decoherence rates are suppressed partially or completely by the effects of decoherence. For large qubit decoherence rates, the qubit excitation probability is greatly reduced close to resonance, where the Rabi frequency $\Omega$ takes its lowest values. The shallow dip in the dash-dotted line in figure 5 occurs because for those frequencies and in the absence of decoherence the maximum amplitude is only reached after

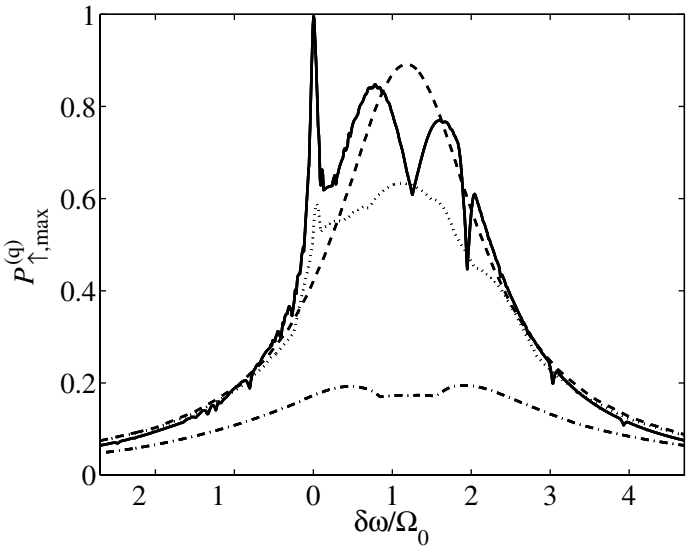


**Figure 5.** Maximum qubit excitation probability $P^{(q)}_{\uparrow,max}$ between $t = 0$ and $20\pi/\Omega_0$. The solid line corresponds to the case of no decoherence. The dotted ($\Gamma^{(q)}_{1,2} = 0.1\Omega_0/2\pi$ and $\Gamma^{(TLS)}_{1,2} = 0.2\Omega_0/2\pi$), dashed ($\Gamma^{(q)}_{1,2} = 0$ and $\Gamma^{(TLS)}_{1,2} = 2\Omega_0$) and dash-dotted ($\Gamma^{(q)}_{1,2} = \Omega_0$ and $\Gamma^{(TLS)}_{1,2} = 0$) lines correspond to different decoherence regimes. $\lambda/\Omega_0 = 2$, $\theta_q = \pi/4$ and $\theta_{TLS} = \pi/5$. $\Gamma^{(\alpha)}_1$ and $\Gamma^{(\alpha)}_2$ are the relaxation and dephasing rates of the subsystem $\alpha$, respectively.

several oscillations, whereas it is reached during the first few oscillations outside that region. For large TLS decoherence rates, the TLS becomes weakly coupled to the qubit, and a single peak is recovered in the qubit dynamics (with a height larger than either the two split peaks). All of these effects are in agreement with the simple picture presented in section 3.

## 5. Experimental considerations

In the early experiments on phase qubits coupled to TLSs [10, 15], the qubit relaxation rate $\Gamma^{(q)}_1$ (∼40 MHz) was comparable to the splitting between the two Rabi peaks $\lambda_{ss}$ (∼20–70 MHz), whereas the on-resonance Rabi frequency $\Omega_0$ was tunable from 30 to 400 MHz (note that, as discussed in section 3, the Rabi frequency cannot be reduced to values much lower than the decoherence rates, or Rabi oscillations would disappear altogether). The large relaxation rates in those experiments would make several effects discussed in this paper unobservable. The constraint that $\Omega_0$ could not be reduced below 30 MHz made the strong-coupling regime, where $\Omega_0 \ll \lambda_{ss}$, inaccessible. The weak-coupling regime, where $\Omega_0 \gg \lambda_{ss}$, was easily accessible in those experiments. However, as can be seen from figure 2, it shows only a minor signature of the TLS. Although the intermediate-coupling regime was also accessible, as evidenced by the observation of the splitting of the Rabi peak into two peaks, observation of the two-photon process and the additional dips of figure 2 discussed above would have required a time at least comparable to the qubit relaxation time. That would have made them difficult to distinguish from experimental fluctuations.

With the new qubit design of [25], the qubit relaxation time has been increased by a factor of 20. The constraint that $\Omega_0$ must be at least comparable to $\Gamma_{1,2}^{(q)}$ no longer prevents accessibility of the strong-coupling regime. Furthermore, since our simulations were run for a period of time corresponding to approximately ten Rabi oscillation cycles, i.e. shorter than the relaxation time observed in that experiment, all the effects that were discussed above should be observable, including the observation of the two-photon peak and the transition from the weak- to the strong-coupling regimes by varying the driving amplitude.

We finally consider one possible application of our results to experiments on phase qubits, namely the problem of characterizing the environment composed of TLSs. As we shall show shortly, characterizing the TLS parameters and the nature of the qubit–TLS coupling are not independent questions. The energy splitting of a given TLS, $E_{\rm TLS}$, can be obtained easily from the location of the qubit-TLS resonance as the qubit energy splitting is varied. One can then obtain the distribution of values of $E_{\rm TLS}$ for a large number of TLSs, as was in fact done in [25]. The splitting of the Rabi resonance peak into two peaks by itself, however, is insufficient to determine the values of $\Delta_{\rm TLS}$ and $\epsilon_{\rm TLS}$ separately. By observing the location of the two-photon peak, in addition to the locations of the two main peaks, one would be able to determine both $\lambda_{\rm cc}$ and $\lambda_{\rm ss}$ for a given TLS, as can be seen from figure 1. Those values can then be used to calculate both $E_{\rm TLS}$ and $\theta_{\rm TLS} \equiv \arctan(\Delta_{\rm TLS}/\epsilon_{\rm TLS})$ of that TLS. The distribution of values of $\theta_{\rm TLS}$ can then be used to test models of the environment, such as the one given in [17] to describe the results of [26].

In order to reach the above conclusion, we have made the assumption that the distribution of values of $\theta_{\rm TLS}$ for those TLSs with sufficiently strong coupling to the qubit is representative of all TLSs. Since it is generally believed that strong coupling is a result of proximity to the junction, the above assumption is quite plausible, as long as the other TLSs share the same nature. Although it is possible that there might be two different types of TLSs of different nature in a qubit's environment, identifying that possibility would also be helpful in understanding the nature of the environment. We have also assumed that $\theta_{\rm q}$ does not take the special value $\pi/2$ (note that, based on the arguments of [17, 26], we are also assuming that generally $\theta_{\rm TLS} \neq \pi/2$). That assumption would not raise any concern when dealing with charge or flux qubits, where both $\Delta_{\rm q}$ and $\epsilon_{\rm q}$ can be adjusted in a single experiment, provided an appropriate design is used. However, the situation is trickier with phase qubits. The results in that case depend on the nature of the qubit–TLS coupling, which we discuss next.

The two mechanisms that are currently considered the most likely candidates to describe the qubit–TLS coupling are through either (i) a dependence of the Josephson junction's critical current on the TLS state or (ii) Coulomb interactions between a charged TLS and the charge across the junction. In the former case, one has an effective value of $\theta_{\rm q}$ that is different from $\pi/2$ (further arguments regarding the value of $\theta_{\rm q}$ are given in [27]), and the assumption of an intermediate value of $\theta_{\rm q}$ is justified. In the case of coupling through Coulomb interactions, on the other hand, one effectively has $\theta_{\rm q} = \pi/2$, and therefore $\lambda_{\rm cc}$ vanishes for all the TLSs. In that case the two-photon peak would always appear at the midpoint (to a good approximation) between the two main Rabi peaks. Although that would prevent the determination of the distribution of values of $\theta_{\rm TLS}$, it would be a strong indication that Coulomb interactions with the charge across the junction are responsible for the qubit–TLS coupling rather than the critical current dependence on the TLS state. Note also that if it turns out that this is in fact the case, and the distribution of values of $\theta_{\rm TLS}$ cannot be extracted from the experimental results, that distribution might be irrelevant to the question of decoherence in phase qubits.

## 6. Conclusion

We have studied the problem of a harmonically driven qubit that is interacting with an uncontrollable TLS and a background environment. We have presented a simple picture to understand the majority of the phenomena that are observed in this system. That picture is composed of three elements: (i) the four-level energy spectrum of the qubit+TLS system, (ii) the basic properties of the Rabi-oscillation dynamics and (iii) the basic effects of decoherence. We have confirmed the predictions of that picture using a systematic numerical analysis where we have varied a number of relevant parameters. We have also found unexpected features in the resonance-peak structure. We have analysed the behaviour of the system and provided simple explanations in those cases as well. Our results can be tested with available experimental systems. Furthermore, they can be used in experimental attempts to characterize the TLSs surrounding a qubit, which can then be used as part of possible techniques to eliminate the TLSs' detrimental effects on the qubit operation.

## Acknowledgments

This work was supported in part by the Army Research Office (ARO), Laboratory of Physical Sciences (LPS), National Security Agency (NSA) and Advanced Research and Development Activity (ARDA) under Air Force Office of Research (AFOSR) contract number F49620-02-1-0334; and also supported by the National Science Foundation grant no EIA-0130383. One of us (SA) was supported by a fellowship from the Japan Society for the Promotion of Science (JSPS).

## References

[1] You J Q and Nori F 2005 *Phys. Today* **58** (11) 42
Makhlin Y, Schön G and Shnirman A 2001 *Rev. Mod. Phys.* **73** 357
[2] Nakamura Y, Pashkin Yu A and Tsai J S 1999 *Nature* **398** 786
[3] Nakamura Y, Pashkin Yu A and Tsai J S 2001 *Phys. Rev. Lett.* **87** 246601
[4] Vion D, Aassime A, Cottet A, Joyez P, Pothier H, Urbina C, Esteve D and Devoret M H 2002 *Science* **296** 886
[5] Yu Y, Han S, Chu X, Chu S-I and Wang Z 2002 *Science* **296** 889
[6] Martinis J M, Nam S, Aumentado J and Urbina C 2002 *Phys. Rev. Lett.* **89** 117901
[7] Chiorescu I, Nakamura Y, Harmans C J P and Mooij J E 2003 *Science* **299** 1869
[8] Pashkin Yu A, Yamamoto T, Astafiev O, Nakamura Y, Averin D V and Tsai J S 2003 *Nature* **421** 823
[9] Yamamoto T, Pashkin Yu A, Astafiev O, Nakamura Y and Tsai J S 2003 *Nature* **425** 941
[10] Simmonds R W, Lang K M, Hite D A, Pappas D P and Martinis J M 2004 *Phys. Rev. Lett.* **93** 077003
[11] You J Q and Nori F 2003 *Phys. Rev.* B **68** 064509
[12] Chiorescu I, Bertet P, Semba K, Nakamura Y, Harmans C J P M and Mooij J E 2004 *Nature* **431** 159
[13] Wallraff A, Schuster D I, Blais A, Frunzio L, Huang R S, Majer J, Kumar S, Girvin S M and Schoelkopf R J 2004 *Nature* **431** 162
[14] Johansson J, Saito S, Meno T, Nakano H, Ueda M, Semba K and Takayanagi H 2006 *Phys. Rev. Lett.* **96** 127006
[15] Cooper K B, Steffen M, McDermott R, Simmonds R W, Oh S, Hite D A, Pappas D P and Martinis J M 2004 *Phys. Rev. Lett.* **93** 180401
[16] Ku L-C and Yu C C 2005 *Phys. Rev.* B **72** 024526
[17] Shnirman A, Schön G, Martin I and Makhlin Y 2005 *Phys. Rev. Lett.* **94** 127002

[18] Faoro L, Bergli J, Altshuler B L and Galperin Y M 2005 *Phys. Rev. Lett.* **95** 046805
[19] Galperin Y M, Shantsev D V, Bergli J and Altshuler B L 2005 *Europhys. Lett.* **71** 21
[20] Ashhab S, Johansson J R and Nori F 2005 *Preprint* cond-mat/0512677
[21] Baym G 1990 *Lectures on Quantum Mechanics* (New York: Addison-Wesley)
[22] Cohen-Tannoudji C, Dupont-Roc J and Grynberg G 1992 *Atom-Photon Interactions* (New York: Wiley)
[23] Slichter C P 1996 *Principles of Magnetic Resonance* (New York: Springer)
[24] Smirnov A Yu 2003 *Phys. Rev.* B **67** 155104
Kosugi N, Matsuo S, Konno K and Hatakenaka N 2005 *Phys. Rev.* B **72** 172509
[25] Martinis J M *et al* 2005 *Phys. Rev. Lett.* **95** 210503
[26] Astafiev O, Pashkin Yu A, Nakamura Y, Yamamoto T and Tsai J S 2004 *Phys. Rev. Lett.* **93** 267007
[27] Zagoskin A M, Ashhab S, Johansson J R and Nori F 2006 *Preprint* cond-mat/0603753